

People and buildings vulnerability to floods in mountain areas

Marco Pilotti, Ph.D.¹; Luca Milanesi, Ph.D.¹; Roberto Ranzi, Ph.D.¹

ABSTRACT

Risk assessment needs rational and quantitative methodologies to describe hazard, vulnerability and exposure. This paper focuses on physical vulnerability functions based on mechanical schemes representing human stability and building structural resistance in a flow. These instruments were used to model the Gleno dam break event that occurred in 1923 in Valle di Scalve (Northern Italy). An innovative modelling approach adapting the domain bathymetry to the potential building collapse is proposed and positively tested.

KEYWORDS

2D model; Buildings vulnerability; Dam break; Flood mapping; People's vulnerability

INTRODUCTION

Hydraulic risk is a combination of hazard, exposure and vulnerability. Accordingly, quantitative procedures are needed to calculate the flow features, to identify the exposed targets (e.g., people, buildings, cars, etc.) and define the potential damage associated to each flow condition. Only this rational roadmap provides objective results so that the related legislative planning instruments can be understood, accepted and shared among stakeholders. The criteria used to assess exposure and vulnerability are still poorly discussed and this study focuses on people's and buildings vulnerability to floods.

Several models of people's vulnerability to floods are available in the literature from both conceptual and experimental studies (e.g., Xia et al., 2014). They are useful to estimate the potential loss of life due to floods (Jonkman et al., 2008). Anyway, these models are mostly empirical and a satisfactory treatment of physical aspects such as the role of local slope and fluid density is still missing. Milanesi et al. (2015) proposed a weakly parametric conceptual model that includes a detailed treatment of these issues. The model, briefly summarized in the following, best matches the available experimental data.

Although the most common method for the estimation of direct damage to buildings is still the application of stage-damage functions (Jongman et al., 2012), structural vulnerability models are available (e.g., Clausen & Clark, 1990) and worth to be investigated. The current study provides a conceptual scheme comparing the actions exerted by the flow on a simplified masonry building with the resistance of the structure itself, considering the potential failure mechanisms of a partly confined wall.

¹ Università degli Studi di Brescia, ITALY, luca.milanesi@unibs.it

These criteria have been applied to the Gleno dam break event which occurred in 1923 with catastrophic consequences in Valle di Scalve, a right tributary of Valle Camonica, drained respectively by the Dezzo and Oglio rivers. The flood took about 45 min to flush the 21 km-long stretch from the dam to the confluence of the rivers at Corna (Darfo). Pilotti et al. (2011) studied the event by a 1D model of the Dezzo river as far as the alluvial fan of Corna. Here a 2D code has been applied to model the flood on the fan, including a dynamic procedure accounting for building collapse. The preliminary results of the model are compared to observed data derived from historical documents.

PEOPLE'S VULNERABILITY TO FLOODS

As proposed by Lind et al. (2004), the human body is represented by a set of cylinders in vertical position on an inclined slope (Fig. 1) and impacted frontally by a steady uniform flow. The body weight W is decomposed in direction normal W_N and parallel W_p to the slope. Considering the pressure distribution of a parallel flow, the buoyancy force B_N is normal to the bed. Since the body stands in vertical position on the slope, it is not normal to the flow field. Neglecting skin friction, the fluid dynamic force R is normal to the body frontal area and it can be decomposed in direction parallel and normal to the slope, giving drag D and lift L forces respectively. Friction T between the soles and the bed is the product of the coefficient μ (0.46, after calibration) and the effective weight w that is the algebraic sum of the forces normal to the slope: W_N , B_N and L

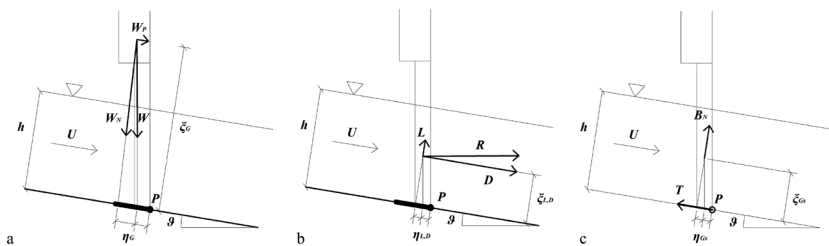


Figure 1: Acting forces and their application points: (a) weight, (b) dynamic actions, and (c) buoyant and friction forces. Partial lateral view of the body. See Milanese et al. (2015) for details on the symbols.

Slipping instability occurs if the sum of the drag force and of the component of weight W_p overcomes friction. Toppling instability occurs if the moment calculated with respect to the pivot point P , in this case the heel, of the component of the weight W_N is exceeded by the destabilizing moments due to lift, drag, buoyancy and the component of the weight W_p . A third condition is introduced to consider drowning by imposing a maximum admissible water depth as a function of the height of the neck. The depth safety limit, as a function of the flow velocity U , is given by the minimum among slipping, toppling and drowning depths (Fig. 2).

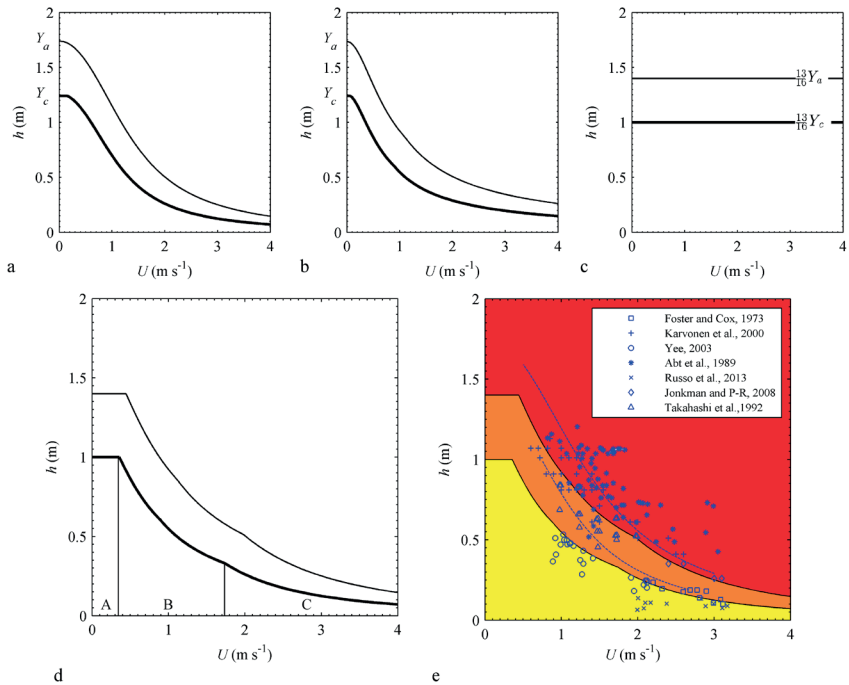


Figure 2; Stability curves for adults ($m=71$ kg, $Y_a=1.71$ m, thin line) and children ($m=22.4$ kg, $Y_c=1.21$ m, thick line): (a) slipping (b) toppling (c) drowning; combined in Fig. (d) ($\rho=1000$ kg/m³ and $\theta=0^\circ$). A, B, and C influence areas in (d) represent respectively the drowning, toppling and slipping controlled areas for children. Fig. (e) shows literature experimental data and the curves by Xia et al. (2014) (dashed). High, medium and low vulnerability are respectively identified by red, orange and yellow. See Milanese et. al. (2015) for details on the cited studies.

BUILDINGS STRUCTURAL VULNERABILITY TO FLOODS

Alpine traditional masonry buildings are modelled using a simple structure with weight-bearing walls. Accordingly, it is subdivided in elementary modules independent from each other, whose stability is assessed with respect to the wall impacted by the flow. Under the action of a horizontal acceleration normal to the wall, the wall flexes out-of-plane, rotating around a horizontal or vertical joint, depending on the constraint exerted by the surrounding walls. The loading force F per unit width is made of a hydrostatic F_{st} and a dynamic F_d term, the latter amplified to represent the impulsive behaviour of the impact (Cross, 1967).

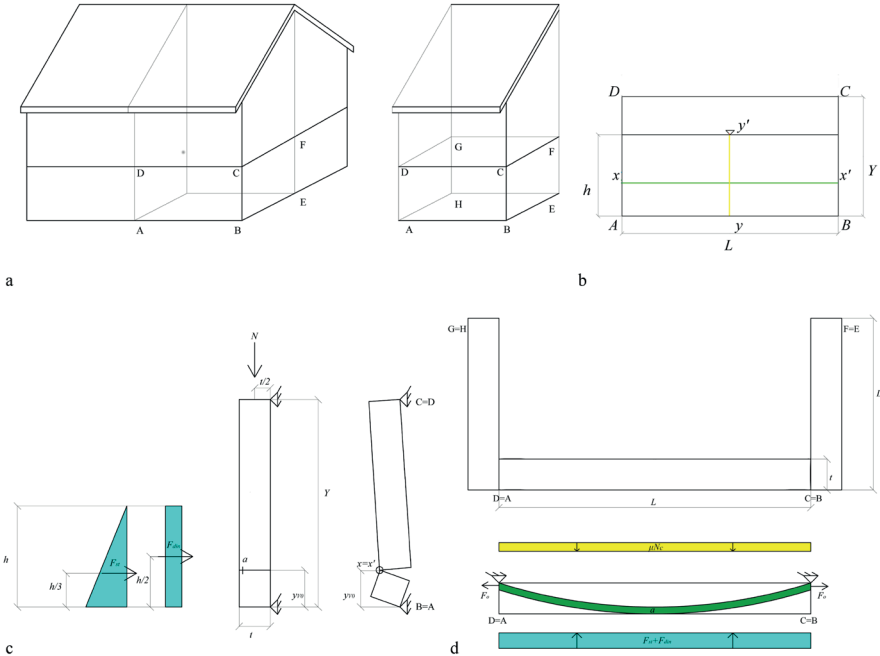


Figure 3: Scheme of the building (a) and detail of the impacted wall with tracks of the failure joints (b). Horizontal (c) and vertical (d) joint failure mechanisms.

The first failure mechanism is modelled considering a vertical strip of the wall of unit width, thickness t , and height Y as a simply supported beam loaded by a trapezoidal pressure distribution. It fails along a horizontal joint of thickness a ($x-x'$, Fig. 3b) if the maximum moment M_{max-h} caused by the flow pressure is greater than the stabilizing moment M_{u-h} due to the vertical loads N .

$$M_{max-h} \geq M_{u-h} \rightarrow M_{max-h} \geq N \left(\frac{t}{2} - \frac{a}{2} \right)$$

Formula 1

The second failure mechanism is modelled by considering the portion of the wall of height h and width L as a laterally simply supported beam. The pressure distribution is uniform and the stability is provided by a resisting arch that transfers the load F_0 on the sidewalls and by the friction force per unit width F_μ at the interface at height h . The vertical joint ($y-y'$, Fig. 3b) triggers if the maximum moment on the beam M_{max-v} is greater than the resisting moment M_{u-v} .

$$M_{max-v} \geq M_{u-v} \rightarrow M_{max-v} \geq F_0 \left(t - \frac{a}{2} \right) + F_\mu \frac{L^2}{8}$$

Formula 2

The limiting stability condition is represented by the horizontal joint mechanism.

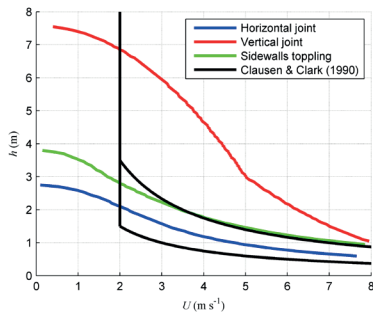


Figure 4: Stability thresholds associated to the described mechanisms calculated for a 2.5 storey building with walls 0.45 m thick.

THE GLENO DAM BREAK TEST CASE

The Digital Terrain Model (DTM) of the domain was derived from LIDAR data, filtered from buildings and vegetation, with 1 m resolution (Source: Italian Ministry of the Environment and Protection of Land and Sea). It was averaged at uniform sized cells of 7.5 m in order to represent buildings and limit the computational effort. The urban area and the path of the Dezzo river in 1923 were reconstructed through historical maps. Because of the lack of quantitative and reliable information regarding the original geometry of the Dezzo river, a rectangular approximation was assumed. The original path was derived from historic maps.

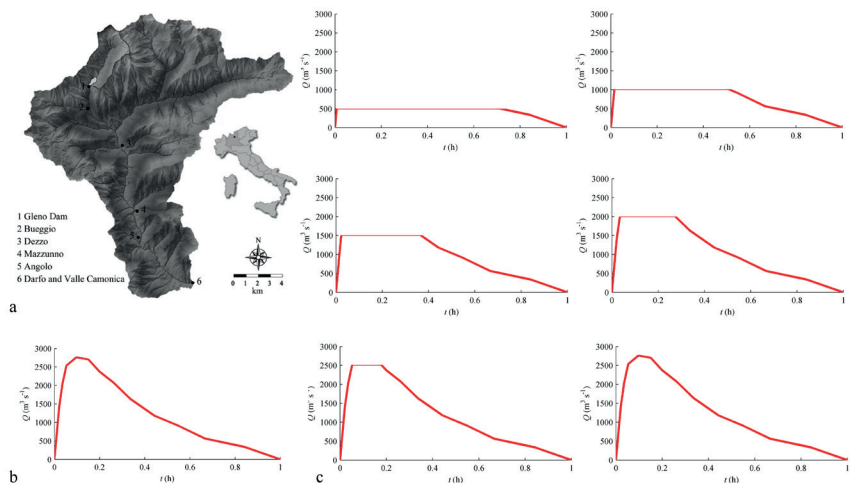


Figure 5: a) Location of the study area. b) Input hydrograph (Pilotti et al., 2011). c) Discretization of the hydrograph for the dynamic approach.

The code used to compute local flow depth and velocity (FLO-2D) solves the full two dimensional (2D) shallow water equations (SWE) on a Cartesian grid using an explicit, central, finite difference numerical scheme along eight flow directions. This software, already applied successfully to the dam break study of Cancano (Pilotti et al., 2014), was chosen also for its compliance with the requirements of the Federal Emergency Management Agency (FEMA) in USA about hydraulic modelling.

Urban flooded domains have uneven roughness and traditional a priori estimates of roughness are not feasible in case of impulsive flood waves affecting significantly the domain morphology and roughness. Accordingly, roughness was assumed constant and calibrated ($k_s=30 \text{ m}^1/\text{s}$) with reference to the depth observed in several points of the domain. It was shown (e.g., Soares-Frazaõ & Zech, 2008) that the presence of buildings as well as their alignment influence the flow field and the flood extent. This is especially true as far as impulsive floods are concerned since their destructive impact on buildings can dynamically alter the bathymetry. Accordingly, in the following two different modelling approaches will be compared: a static one, keeping the buildings in their initial position during the entire simulation based on the hydrograph in Fig. 5b, and a dynamic one, provided by a series of

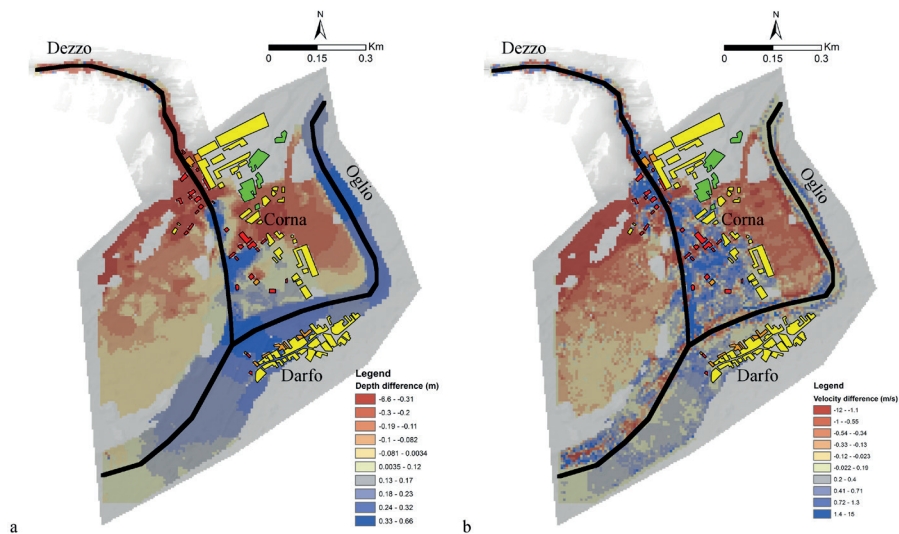


Figure 6: Differences in maximum flow depth (a) and velocity (b). Blue indicates that the dynamic simulation provides values greater than the ones from the static model; red colour indicates the opposite situation. White indicates substantial equality between the results of the two approaches. GREEN: flooded buildings; YELLOW: submerged buildings; ORANGE: partly destroyed buildings; RED: destroyed buildings.

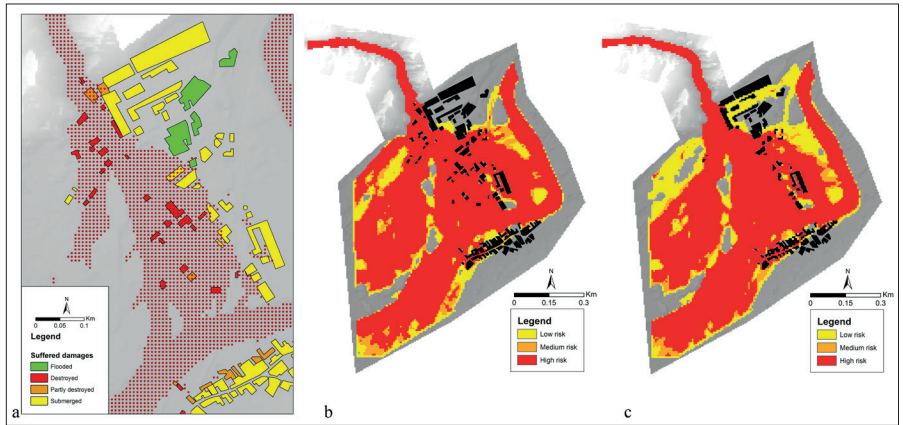


Figure 7: (a) Validation of the structural vulnerability model; the red dots indicate where, according to the presented model (section 2), buildings would be destroyed by the flow in the dynamic approach. Risk to people maps from the static (b) and dynamic (c) approaches.

simulations of partial hydrographs (Fig. 5c). At the end of each partial simulation, the buildings destroyed according to the structural vulnerability model are removed from the domain and a roughness value $k_s=10 \text{ m}^{1/3}/\text{s}$ is assigned to the area previously covered by the structure to represent the presence of debris. The following simulation is then run from the beginning of the hydrograph with the updated bathymetry.

RESULTS AND CONCLUSIONS

The main difference between the two simulations is related to the lateral spread of the flow due to the interaction with the buildings (Fig. 6). The static simulation estimates greater depths and velocities in the lateral areas of the fan because of the diffusion caused by buildings. On the contrary, with the dynamic approach the flow is more concentrated along the centre of the domain because of the gradual removal of the destroyed structures based on the vulnerability model, whose reliability is demonstrated in Fig. 7a. The comparison of the estimated flow depths with data from historical images proves that the dynamic approach is more accurate than the static one (RMSE=0.69 m and 0.78 m respectively). Risk was classified by the vulnerability criterion for people, whose exposition was considered unitary. As usual in extreme events, Figs. 7b and 7c show a strong polarization toward high risk areas. The main advantages of the model of people vulnerability is the direct dependency of the thresholds from fluid density and local slope that are key parameters especially in mountain areas. Similarly, on the contrary of empirical formulae (e.g., Clausen & Clark, 1990), the physically based model of buildings structural vulnerability can be adapted to different structural typologies. Finally, the dynamic modelling of extreme events allows a more realistic hazard assessment and an accurate estimate of the consequences on structures. The simple physically based procedures presented in this study allow a reliable reproduction of flood

events and a more objective representation of risk that might guarantee comprehensibility and acceptability of the related plans and constraints to the stakeholders.

REFERENCES

- Clausen L., Clark P. (1990). The development of criteria for predicting dam break flood damages using modeling of historical dam failures. Proc. Int. Conf. on River Flood Hydraulics, W. White (ed.), Wiley, U.K, 369–380.
- Cross, R.H. (1967). Tsunami Surge Forces. Journal of the Waterways and Harbors Division 93(4): 201-231.
- Jongman B., Kreibich H., Apel H., Barredo J. I., Bates P. D., Feyen L., Gericke A., Neal J., Aerts J.C.J.H., Ward P.J. (2012). Comparative flood damage model assessment: towards a European Approach. Nat. Hazards Earth Sys. 12: 3733–3752.
- Jonkman S.N., Vrijling J.K., Vrouwenvelder A.C.W.M. (2008). Methods for the estimation of loss of life due to floods: a literature review and a proposal for a new method. Nat Hazards 46: 353-389.
- Lind N., Harford D., Assaf H. (2004). Hydrodynamic models of human stability in a flood, J. Am. Water Resour. As. 40(1): 89–96.
- Milanesi L., Pilotti M., Ranzi R. (2015). A conceptual model of people's vulnerability to floods. Water Resour. Res. 51(1):182-197.
- Pilotti M., Maranzoni A., Tomirotti M., Valerio G. (2011). The 1923 Gleno dam-break: case study and numerical modelling. J. Hydraul. Eng. 137(4): 480-492.
- Pilotti M., Maranzoni A., Milanesi L., Tomirotti M., Valerio G. (2014). Dam-break modeling in alpine valleys. J. Mt. Sci. 11(6): 1429-1441.
- Soares-Frazão S., Zech Y. (2008). Dam-break flow through an idealized city. J. Hydraul. Res. 46(5): 648-658.
- Xia J., Falconer R.A., Wang Y., Xiao X. (2014). New criterion for the stability of a human body in floodwaters. J. Hydraul. Res. 52(1): 93-104.